Journal of Long-Term Effects of Medical Implants, 6(3&4):143–155(1996)

Cyclic Fatigue of Hydroxyapatite-Coated Titanium Alloy Implant Material—Effect of Crystallinity

*Shafeek Ashroff, M.S.,[1] Stan A. Napper, Ph.D.,[1] Paul N. Hale, Jr., Ph.D.,[1] Upali Siriwardane, Ph.D.,[1] and Debi P. Mukherjee, Sc.D.[2]**

[1]Departments of Biomedical Engineering and Chemistry, Louisiana Technical University, Ruston, Louisiana 71272; [2]Department of Orthopædic Surgery, Louisiana State University Medical Center, 1501 Kings Highway, Shreveport, Louisiana 71130

* To whom all correspondence should be addressed.

Manuscript Received: July 30, 1996
Manuscript Accepted: August 20, 1996

ABSTRACT: Titanium alloy (ASTM F-136) rods were coated with hydroxyapatite (HA) of 3 levels of crystallinity, which were determined by X-ray diffraction (XRD) analysis to be 60.5%, 52.8%, and 47.8%. Fourier Transform Infrared (FTIR) spectroscopy analysis showed the removal of the hydroxyl and carbonate groups as compared to the original HA powder. It appears that these changes are caused by the high temperature plasma spray coating process. Cyclic fatigue testing in a lactated Ringer's solution to 5 million cycles showed no statistical difference in calcium dissolution among the 3 crystalline levels, whereas phosphorus dissolution was lowest from the highest crystalline coating sample. The mechanical properties, however, did not change in response to fatigue loading.

KEY WORDS: hydroxyapatite, cyclic fatigue, crystallinity, stability, titanium alloy.

I. INTRODUCTION

Hydroxyapatite coating of dental and orthopædic implants was found to be biocompatible and osteoconductive in several animal and clinical studies.[1-8] Short-term (2–3 year) experience with HA-coated implants in orthopædic applications has shown good bone apposition.[9,10] Clinical data[11,12] with HA-coated dental implants over 5- and 8-year periods indicates that implants made recently (1989–1991) had a superior performance than those made earlier (1985–1988) and exhibited insignificant coating disintegration. A number of studies reported the need for proper characterization of the HA coating—thickness, implant design, and type of

1050-6934/96 $5.00

bone (maxilla vs. mandible)—affecting the stability of the HA coating in long-term use.[13-21] Scanning electron microscopy of failed HA-coated dental implants from clinical use showed that failure was primarily located at the HA–metal interface, not the HA–bone interface.[22] *In vitro* fatigue studies with HA-coated titanium metal alloy materials showed that cyclic fatigue caused widening of microcracks and dissolution of calcium and phosphate.[23-25]

We reported results of cyclic fatigue testing of 5 commercial dental implants immersed in a lactated Ringer's solution.[26-27] We concluded that there was widening of microcracks and dissolution of calcium and phosphate coating from 5 million cycles of cyclic loading, which simulated about 5 years of *in vivo* life. To our knowledge, *in vitro* fatigue studies on well-characterized HA-coated dental implants with different levels of crystallinity of the HA coating have not been widely reported. Such studies are important to gain insight into how stability of the HA coating is influenced by crystallinity levels when subjected to cyclic fatigue loading.

The objective of the current study is to test the hypothesis that HA-coated implants of higher crystallinity will be stable and that calcium and phosphate dissolution will be minimal when these samples are subjected to fatigue loading.

II. MATERIALS AND METHODS

ELI (extra low interstitial)-grade Ti-6A1-4V rods were machined to 19.67 mm in length and 4 mm in diameter and HA coated by a plasma spray process.

A. Coating Application

HA powder conforming to ASTM F1185-88 specifications was plasma-sprayed onto the Ti-6A1-4V implants as 50 μm thick HA coatings at 3 crystallinity levels (Bio-Coat, Inc., Southfield, Michigan). The crystallinity of the coating was varied by changing the distance between the plasma spray gun and the substrate. For better adhesion, the surfaces of the specimens were roughened by grit-blasting prior to plasma-spraying. Each group had 8 samples, the uncoated samples with and without grit blasting serving as controls.

In addition to these samples, flat Ti-6A1-4V coupons of dimensions 25 × 25 × 3.2 mm were also coated with HA of the same crystallinity levels as were the rods. These coupons underwent the identical manufacturing and processing procedures as did the cylinders. Each group had 6 coupons, which were used for XRD, FTIR, and coating dissolution analyses.

B. Coating Characterization

The HA original powder and the coatings on the test samples were characterized using XRD and FTIR. The percentage by weight of the crystalline phases identified as HA, α-TCP, ß-TCP, and CaO in the plasma-sprayed coatings were determined from the XRD analysis. A standard Bragg-Brentano diffractometer equipped with a graphite monochromator (Cu-Kα radiation of wavelength 1.54 A°) was employed. Diffraction scans were run with a tube voltage of 40kV and a tube current of 28mA. Each diffraction scan was run from 20°–60° two-theta with a step of 0.02° and a scan time at each increment of 2 seconds. A 1.0° incident beam divergence and a 0.2° receiving slit were used.

The infrared spectra were obtained on the HA original powder as well as on coatings scraped off the Ti-6A1-4V coupons. Coatings weighing about 1.5–3.0 mg were embedded in 300 mg KBr pellets hand-pressed hydraulically at 20 tons. The spectra were obtained using a Mattson 2020 Galaxy Series FTIR spectrometer, which was operated with a 10-minute scanning time for the 4000–400 cm^{-1} range.

C. Fatigue Testing

A special sample holder, which was previously described elsewhere,[26] is shown in Figure 1. The test samples were immersed in a lactated Ringer's solution of pH 7.0. This sample holder, holding 1 group of 8 samples, was loaded in a biaxial Instron Mechanical Tester Model 1321. Loading of individual samples in the loading fixture was checked by inserting a pressure-sensitive film between the top of the samples and the cap of the fixture. Eight samples were then cycled between 240 and 480 pounds load of compression, i.e., 30–60 lbs/sample, at an ambient temperature and a frequency of 10 Hz for approximately 5 million cycles, to simulate 5 years of *in vivo* loading. Fatigue testing each group of samples took about 2 weeks, because the machine ran only in the daytime.

D. Coating Dissolution Analyses

Calcium (Ca) and phosphate (P) assays were performed on the lactated Ringer's immersing solutions after completion of the fatigue tests to determine any dissolution of coating. One coupon from each group was simultaneously immersed in the same volume of lactated Ringer's solution of pH 7.0 for 2 weeks, then analyzed for Ca and P ion dissolutions. These samples served as controls for the fatigued samples.

The amount of calcium eluted from the samples was measured in triplicate by flame atomic absorption spectrometry using a Perkin-Elmer Model 306 spectro-

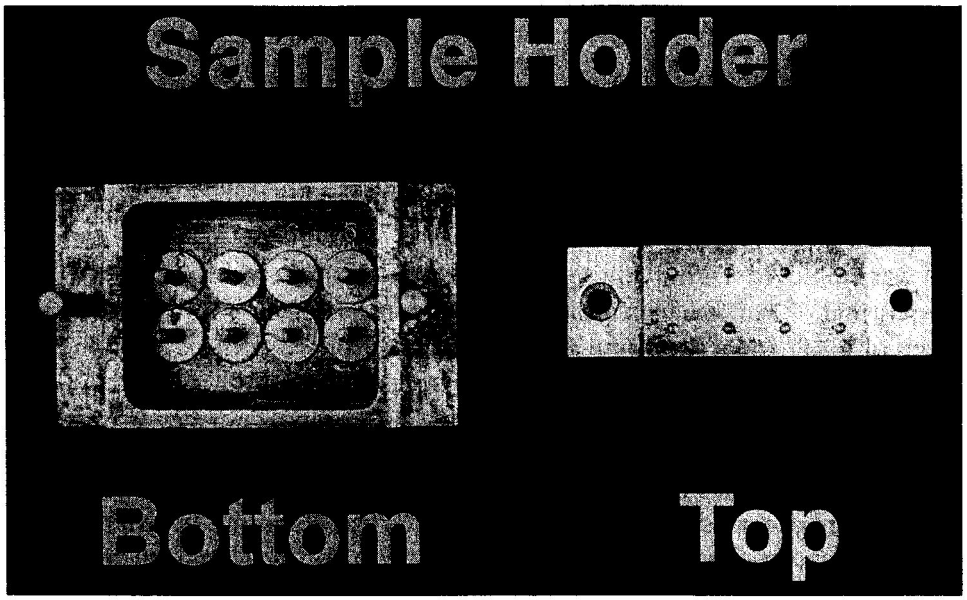

FIGURE 1. Sample holder for 8 specimens.

photometer. The phosphate content of the immersing solutions was colorimetrically determined in triplicate using a Hitachi U-1100 spectrophotometer.

E. Strength Testing

Both fatigued and unfatigued implants were tested in compression to determine their yield strengths using the Instron Mechanical Tester Model 1321. An IBM-AT PC connected to the machine acquired the applied load and corresponding change in length through an A/D board. The initial length and the cross-sectional areas of the samples were used to calculate the stress and strain values. Stress–strain diagrams were plotted for each sample, and yield strength and yield strain of the material were obtained from the plots.

III. RESULTS

The XRD analyses results are shown in Table 1. The crystallinity levels of the 3 groups were 60.5% (Group 1), 52.8% (Group II), and 47.8% (Group III). Statistical analysis showed a significant difference in crystallinity among the different groups ($p < .05$) (Table 2).

TABLE 1
Quantitative Phase Analysis of HA Coatings on Ti-6A1-4V Coupons

Sample ID	% HA	% α-TCP	% ß-TCP	% CaO	% Crystallinity
HA Starting Powder	99.6 ± 0.9	0.0 ± 0.0	0.4 ± 0.1	0 ± 0	100.0 ± 0.9
Group I - Coupon A	58.0 ± 3.7	0.1 ± 0.6	3.3 ± 1.5	0 ± 0	61.3 ± 4.0
Group I - Coupon B	53.9 ± 3.7	0.5 ± 0.6	5.2 ± 1.5	0 ± 0	59.6 ± 4.0
Group II - Coupon A	47.2 ± 3.8	0.1 ± 0.7	4.6 ± 1.5	0 ± 0	51.9 ± 4.1
Group II - Coupon B	48.1 ± 3.7	0.5 ± 0.6	5.1 ± 1.5	0 ± 0	53.7 ± 4.1
Group III - Coupon A	43.0 ± 3.8	0.2 ± 0.7	5.0 ± 1.6	0 ± 0	48.2 ± 4.2
Group III - Coupon B	43.8 ± 1.0	0.0 ± 0.0	3.5 ± 0.4	0 ± 0	47.3 ± 1.0

The XRD pattern of the original HA powder used in the study is shown in Figure 2. Minimal line broadening is observed in the diffractogram, indicating a well-crystallized material. The flat baseline of the diffraction pattern also indicates a highly crystalline material with little or no amorphous content. The four strongest lines in this pattern are 002, 211, 112, and 300 reflections, corresponding to 25.9°, 31.7°, 32.0°, and 32.8° 2-theta, respectively. This diffractogram could be matched with the diffraction data of standard synthetic HA from the Joint Committee for Powder Diffraction Standards (JCPDS card number 9-0432).

The diffraction pattern obtained from the HA coating from Group I is shown in Figure 3(a). Peak positions for all the groups—HA, α-TCP, ß-TCP, and CaO—matched those of the HA original powder, although there were alterations in the diffraction pattern induced as a result of the coating process. A well-defined flat baseline no longer existed for the diffraction pattern obtained from the coating. It was replaced instead by a nondefined baseline, or "glass bulge," characteristic for amorphous materials. The diffraction patterns from the other two groups are shown in Figures 3(b) and 3(c).

TABLE 2
Statistical Analysis of the XRD Data

Sample ID	Mean Crystallinity (%)	Standard Deviation	t-test Significance	p-value
Group I	60.5	1.2	-	-
Group II	52.8	1.3	YES	0.0252
Group III	47.8	0.6	YES	0.0057

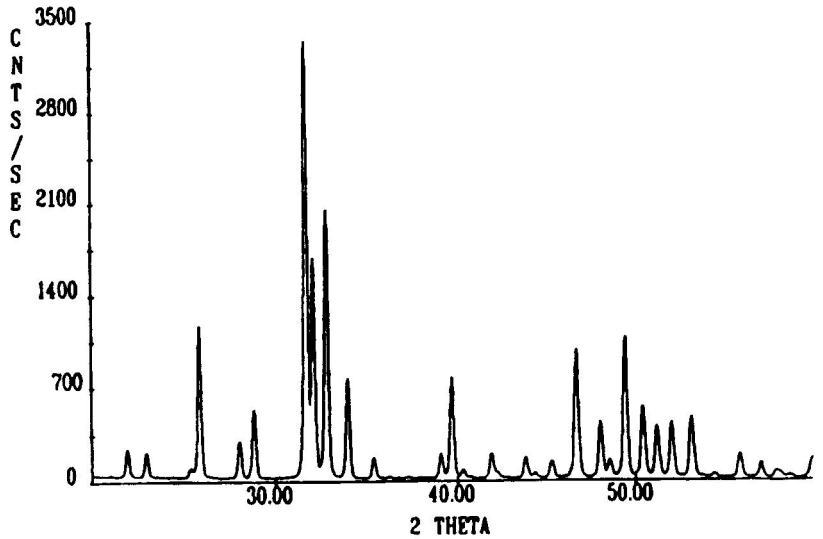

FIGURE 2. XRD pattern of HA original powder.

Infrared spectra of the HA original powder and HA coatings scraped off the coupons showed absorption bands characteristic of P-O and O-H bonds. The infrared spectrum of the HA original powder (see Fig. 4 on page 150) shows that absorption bands characteristic of P-O bonds appear at 1045, 965, 599, and 475 cm^{-1}.

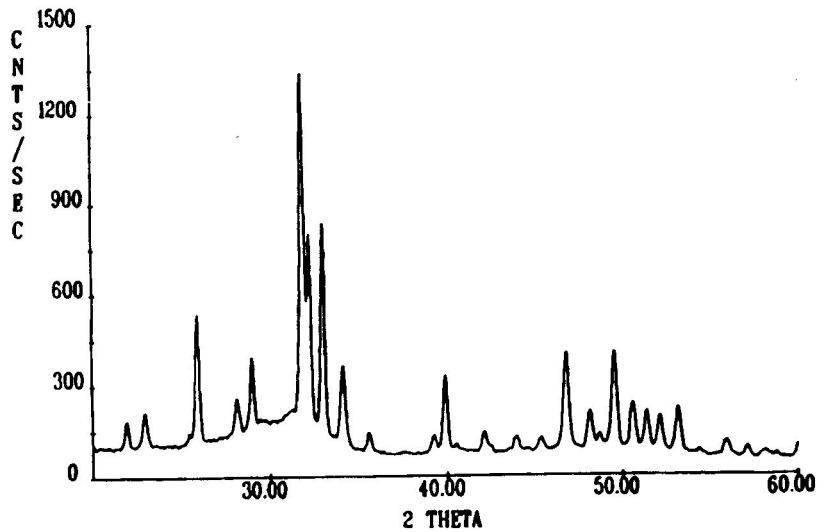

FIGURE 3(a). XRD pattern of HA coating from Group I.

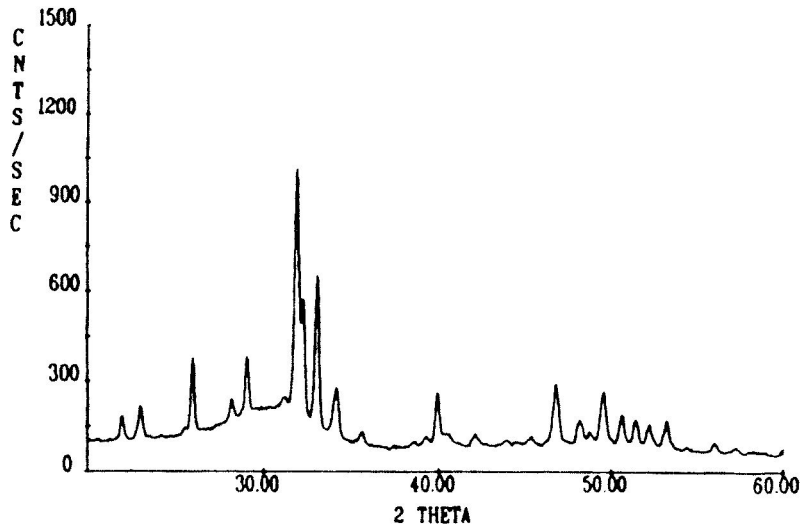

FIGURE 3(b). XRD pattern of HA coating from Group II.

The absorption band at 633 cm^{-1} is indicative of the OH^- liberation peak (υ_1). The OH^- stretching peak (υ_S) at 3570 cm^{-1} was obscured in the spectrum because of noise. A slight carbonate contamination in the HA original powder was seen from the absorption bands at 842 and 1400 cm^{-1}.

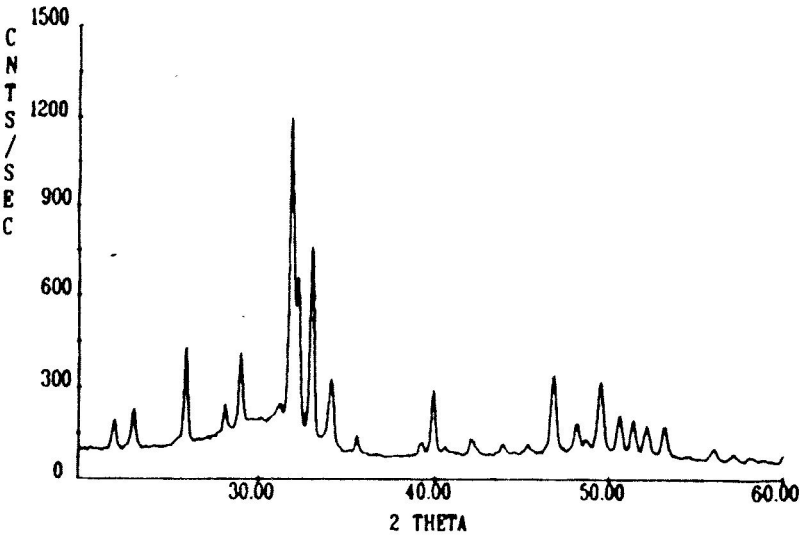

FIGURE 3(c). XRD pattern of HA coating from Group III.

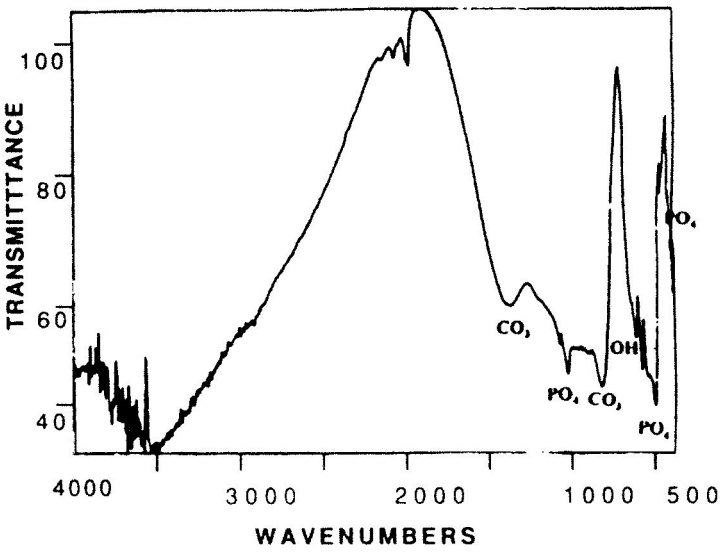

FIGURE 4. FTIR spectrum of HA original powder.

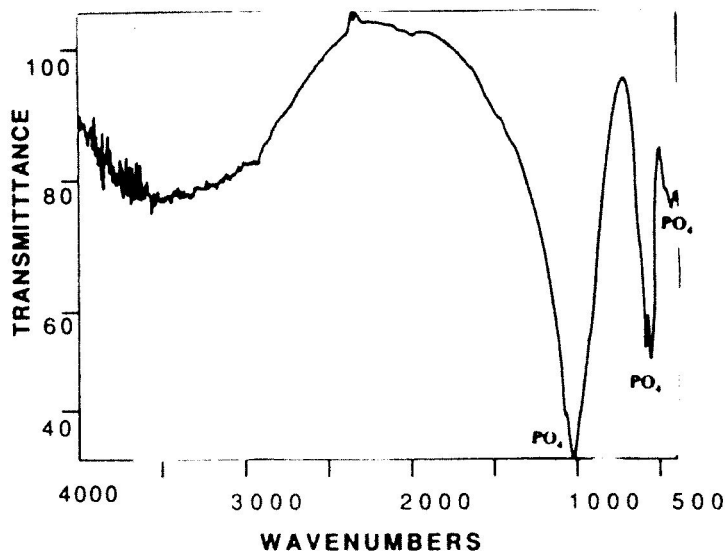

FIGURE 5. FTIR spectrum from Group I.

The infrared spectrum of coating from the Group I coupon is represented in Figure 5. The phosphate vibrations of the HA original powder remained in the HA coatings. The OH^- absorption peak at 633 cm^{-1} disappeared in the spectra obtained from the coatings, indicating dehydroxylation of the HA. As observed in the spectrum of HA original powder, the OH^- absorption peak at 3570 cm^{-1} was also obscured in all the spectra of HA coatings as a result of noise. The CO_3^{2-} absorption peaks at 842 and 1400 cm^{-1} disappeared in the spectra of HA coatings, indicating absence of the carbonate ions in the coatings.

Comparison of the 500–700 cm^{-1} range between the spectra made on the coatings and the standard spectra of oxyhydroxyapatite indicated that the coating contains oxyhydroxyapatite. This finding is in agreement with that reported by Ducheyne et al.[20]

Fatigue testing of each group of samples took approximately 2 weeks to complete. The intensity of the pressure-sensitive films indicated that the total applied load was equally shared by the 8 rods. The results of measurements of Ca concentration in the lactated Ringer's solutions are shown in Table 3. Statistical analysis by Analysis of Variance (ANOVA) did not show any difference in dissolution in Ca among all the samples ($p = 0.20$).

The results of the phosphate dissolution analysis are shown in Table 4. Phosphorus release showed significant differences among the samples ($p < .0001$), the highest crystalline samples showing the least amount of release, and the nonfatigued coupons showing a higher P release than that from fatigued rods; the reason for this is not clear.

TABLE 3
Calcium Dissolution

Sample #	Ca Conc. (ppm)			Ca Conc. (ppm/ mm^2)			Average Ca release (ppm/ mm^2)
	#1	#2	#3	#1	#2	#3	
Group I - Rod	4.12	5.13	19.00	0.0164	0.0204	0.07550	0.037 (±0.033)
Group II - Rod	6.00	19.00	19.30	0.0238	0.0755	0.07660	0.059 (±0.030)
Group III - Rod	8.62	22.88	19.75	0.0342	0.0909	0.07840	0.068 (±0.030)
Group I - Coupon	5.37	17.63	15.75	0.0083	0.0273	0.02441	0.020 (±0.010)
Group II - Coupon	3.00	20.88	22.75	0.0047	0.0324	0.03530	0.024 (±0.017)
Group III - Coupon	6.37	32.25	28.75	0.0099	0.0500	0.04460	0.035 (±0.022)

[a] Surface area of rods = 251.82 mm^2
[b] Surface area of coupons = 645.16 mm^2
[c] ( ) Standard deviation

TABLE 4
Phosphorus Dissolution

Sample #	P Conc. (ppm)			P Conc. (ppm/mm²)			Average P conc. ppm/mm²
	#1	#2	#3	#1	#2	#3	
Group I - Rod	0.419	0.410	0.383	0.0017	0.0016	0.0015	0.0016 (±.0001)
Group II - Rod	0.555	0.813	0.928	0.0022	0.0032	0.0037	0.0030 (±.0007)
Group III - Rod	0.912	1.223	1.200	0.0039	0.0049	0.0048	0.0045 (±.0006)
Group I- Coupon	3.054	3.280	3.381	0.0048	0.0051	0.0052	0.0050 (±.0003)
Group II- Coupon	3.609	3.690	4.062	0.0056	0.0057	0.0063	0.0060 (±.0004)
Group III - Coupon	3.746	4.100	4.198	0.0058	0.0064	0.0065	0.0060 (±.0004)

The stress–strain diagrams of all the samples were similar. Yield strengths of the samples were within 10% of the ASTM value of 827 MPa (Table 5). These results indicate that fatigue did not have a significant effect on the mechanical properties of the HA-coated Ti-6A1-4V alloy substrate.

IV. DISCUSSION

Structural changes of HA coating resulting from the plasma spray process have been reported by Ducheyne et al.[20] These structural and compositional alterations

TABLE 5
Mechanical Properties of the Ti-6A1-4V Implants

Sample ID	Yield Strength (MPa)	Yield Strain (%)
Uncoated & Non Grit-blasted Sample 1	771.43	15
Uncoated & Non Grit-blasted Sample 2	846.15	18
Uncoated & Grit-blasted Sample 1	809.52	16
Uncoated & Grit-blasted Sample 2	836.34	20
HA-coated Rod Group I - Sample 1	823.81	16
HA-coated Rod Group I - Sample 2	-	-
HA-coated Rod Group II - Sample 1	828.57	18
HA-coated Rod Group II - Sample 2	846.15	19
HA-coated Rod Group III - Sample 1	838.01	16

may have been due to extreme temperatures of the plasma spray process. The XRD data obtained in this study indicated that changing the crystallinity of the coatings resulted in a change in the percentage of HA in the coatings. There was no significant difference in the composition of α-TCP, ß-TCP, in the coatings. The XRD patterns obtained in this study for the original powder and the coatings confirmed the presence of a clearly visible HA crystal structure. However, the diffractograms of the coatings indicated that considerable amounts of amorphous material were created by the coating process. This was supported by the drop in crystallinity in the coatings from that of the HA original powder.

FTIR analysis combined with XRD yielded valuable information about the process-induced compositional changes that resulted from plasma-spraying of HA. The broad, featureless band seen in the phosphate region of the spectra of the HA coatings is characteristic of amorphous calcium phosphates. The OH^- band at 633 cm^{-1} observed in the FTIR spectrum of the HA starting powder disappeared in the spectra of the coatings, indicating loss of hydroxyl groups in the HA coatings. Ducheyne et al[20] reported the possible transformation of HA to oxyhydroxyapatite in the coatings as a result of the high temperature involved in the plasma spray process. The OH^- band at 3570 cm^{-1} was not seen in any of the spectra because of high background noise, so definitive conclusions cannot be drawn regarding this absorption band. However, the absorption bands observed at 842 and 1400 cm^{-1} in the spectrum of the HA original powder might indicate a slight carbonate contamination, which disappeared in the spectra of the coatings.

The Ca dissolution data showed no difference in dissolution among the samples, but P analysis showed that the highest crystalline sample had the lowest amount of dissolution. Nevertheless, all rods and coupons showed some Ca and P dissolution.

The data obtained from the mechanical strength determinations indicate that cyclic fatigue loading did not affect the mechanical strength of the implants. Shults[25] reported a 15% decrease in strength for the grit-blasted samples, but this was not observed in our study.

V. CONCLUSIONS

Based on our results we concluded:

1. XRD analysis indicated a significant difference in the degree of crystallinity among the HA-coated samples.
2. High temperature used in the plasma-spray process affected the composition of the HA coatings. FTIR analysis indicated a decrease in hydroxyl and carbonate ions and the presence of oxyhydroxyapatite in the coatings.
3. Dissolution of Ca was not significantly different among the samples, whereas the highest crystalline coating showed minimal P dissolution.

4. Cyclic fatigue loading did not affect the mechanical strength of the HA-coated implants.

ACKNOWLEDGMENTS

The authors wish to thank Lambda Research, Inc., Cincinnati, Ohio, for its help with the X-ray diffraction work; and Bio-Coat, Southfield, Michigan, for HA coating the samples. No benefits have been received or will be received from a commercial party related directly or indirectly to the subject matter of the paper.

REFERENCES

(1) Soballe, K., Hansen, E. S., Rasmussen, A. B., Jorgensen, P. H., and Bunger, C., Tissue ingrowth into titanium and hydroxyapatite-coated implants during stable and unstable mechanical conditions, *J. Orthop. Res.*, **1992**: 10(2):285–299.

(2) Ravagioli, A., Krajewski, A., Biasini, V., Martinetti, R., Managano, C., and Venni, G., Interface between hydroxyapatite and mandibular human bone tissue, *Biomaterials*, **1992**: 13:162–167.

(3) Hayashi, K., Imadome, T., Mashima, T., and Sugioka,Y., Comparison of bone–implant interface shear strength of solid hydroxyapatite and hydroxyapatite-coated titanium implants, *J. Biomed. Mater. Res.*, **1993**: 27:557–563.

(4) Jansen, J. A., Van der Waerden, J. P. C. M., and Wolke, J. G. C., Histologic investigation of the biologic behavior of different hydroxyapatite plasma-sprayed coatings in rabbits, *J. Biomed. Res.*, **1993**: 27:603–610.

(5) Jarcho, M., Retrospective analysis of hydroxyapatite development for oral implant applications, *Dental Clinics No. Am.*, **1992**: 36:19–26.

(6) Whitehead, R. Y., Lacefield, W. R., and Lucas, L. C., Structure and integrity of a plasma sprayed hydroxyapatite coating on titanium, *J. Biomed. Mater. Res.*, **1993**: 27:1501–1507.

(7) de Groot, K., *Bioceramics of Calcium Phosphate*, Boca Raton, FL: CRC Press, 1983.

(8) de Groot, K., Effect of porosity and physicochemical properties on the stability, resorption, and strength of calcium phosphate ceramics, *Ann. NY Acad. Sci.*, **1988**: 523:227–233.

(9) D'Antonio, J. A., Capello, W. N., Crothers, O. D., Jaffe, W. L., and Manley, M. T., Early clinical experience with hydroxyapatite-coated femoral implants, *J. Bone Joint Surg.*, **1992**: 76-A(7):995–1008.

(10) Geesink, R. G. T., Hydroxyapatite-coated total hip prostheses: Two-year clinical and roentgenographic results of 100 cases, *Clin. Orthop. Related Res.*, **1990**: 261:39–58.

(11) Kent, J. N., Block, M. S., Finger, I. M., Guerra, L., Larsen, H., and Misick, D. J., Biointegrated hydroxyapatite-coated dental implants: 5 year clinical observations, *JADA*, **1990**: 121:138–144.

(12) Block, M. S. and Kent, J. N., Cylindrical HA-coated implants—8 year observations, *Compend. Contin.*, **1993**: Supp 15:S526–S532.

(13) James, R., HA-coated root-form implants—Is there cause for concern?, *Dental Implantol. Update*, **1993**: 4(5):37–42.

(14) Lacefield, W. R., Hydroxyapatite coatings, *Ann. NY Acad. Sci.*, **1988**: 523:72–80.

(15) Kay, J. F., Calcium phosphate coatings for dental implants: Current status and future potential, *Dental Clinics No. Am.*, **1992**: 36:1–18.

(16) Koeneman, J., Lemons, J., Ducheyne, P., Lacefield, W., Magee, F., Calahan, T., and Kay, J., Workshop on characterization of calcium phosphate materials, *J. Appl. Biomater.*, **1990**: 1:79–90

(17) Cook, S. D., Thomas, K. A., and Kay, J. F., Experimental coating defects in hydroxyapatite-coated implants, *Clin. Orthop.*, **1991**: 265:280–290.

(18) Prevey, P. S. and Rothwell, R. J., X-ray diffraction characterization of percentage crystallinity and contaminants in plasma-sprayed hydroxylapatite coatings, *Characterization and Performance of Calcium Phosphate Coatings for Implants*, ASTM STP 1196, Philadelphia: American Society for Testing and Materials, 1993.

(19) Ducheyne, P., Raemdonck, W. V., Heughebaert, J. C., and Heughebaert, M., Structural analysis of hydroxyapatite coating on titanium, *Biomaterials*, **1986**: 7:97–103.

(20) Ducheyne, P., Cuckler, J., Radin, S. R., and Nazar, E., Plasma sprayed calcium ceramic linings on porous metal coatings for bone ingrowth, *Handbook of Bioactive Ceramics III*, Boca Raton, FL: CRC Press, 1990; 123–132.

(21) Meffert, R. M., Maxilla vs. mandible— Why use HA?, *Compend. Contin. Edu. Dent.*, **1993**: Suppl 15:S533–S538.

(22) Krauser, J. T., Bertholdt, P., Tammary, I., and Seckinger, R., A scanning electron microscopy study of failed root from dental implant, *J. Dental Res.*, **1991**: 65:274.

(23) Kummer, F. J. and Jaffe, W. L., Stability of a cyclically loaded hydroxyapatite coating: Effect of substrate material, surface preparation, and testing environment, *J. Appl. Biomater.*, **1992**: 3:211–215.

(24) Shults, R. R., A characterization of hydroxylapatite coatings on titanium alloy implant material before and after fatigue, MS Thesis, Department of Biomedical Engineering, University of Memphis, Memphis, TN, 1992.

(25) Shults, R. R., Mukherjee, D. P., and Ray, J. D., A study of fatigue properties of hydroxyapatite coated titanium alloy implant materials, *Transactions of the 20th Annual Meeting of the Society for Biomaterials*, **1994**: 17:332.

(26) Mukherjee, D. P., Wittenberg, J. M., Rogers, S., Kruse, R., and Albright, J. A., Surface changes of hydroxyapatite coated dental implants after cyclic loading, *Proceedings of the 20th Annual Meeting of the Society for Biomaterials*, **1994**: 17:7.

(27) Mukherjee, D. P., Wittenberg, J. M., Rogers, S. H., Kruse, R. N., and Albright, J. A., A fatigue study of hydroxyapatite coated dental implants, *Transactions of the 21st Annual Meeting of the Society for Biomaterials*, **1995**: 18:283.